THE ANNALS OF "DUNĂREA DE JOS" UNIVERSITY OF GALAŢI
FASCICLE V, TECHNOLOGIES IN MACHINE BUILDING,
ISSN 1221- 4566, 2017

NATURAL CONVECTION IN THE BOUNDARY LAYER OF A VERTICAL WALL OF CONSTANT MASS FLUX AND TEMPERATURE EMBEDDED IN A DARCY MASS STRATIFIED POROUS MEDIUM

Maria Neagu[1]

[1]"Dunărea de Jos" University of Galaţi, Manufacturing Engineering Department, Galaţi, România
Maria.Neagu@ugal.ro

ABSTRACT

This paper presents the analysis of the natural convection in the boundary layer of a vertical impermeable semi-infinite wall of constant mass flux and temperature embedded in a Newtonian fluid-saturated Darcy mass-stratified porous medium. Using the scale analysis method, this work determines the two possible successions of the heat and mass driven convection regimes that attain the equilibrium state along the wall. The finite difference method applied to the mathematical model verifies these successions for two particular parameter sets.

KEYWORDS: finite difference method, natural convection, porous medium, scale analysis

1. INTRODUCTION

A vertical impermeable semi-infinite wall embedded in a Newtonian fluid-saturated porous media triggers a natural convection process that received a great consideration from the scientific community in the last decades [1−14] due to its practical applications: materials processing, geothermal engineering, food processing, drying of porous solids, cooling of nuclear reactors, etc.

Depending on the specific application, the scientists considered different wall properties: a constant [1,2] or a variable [3,4] temperature, a constant or a variable [5] heat flux, while the concentration of a certain constituent at the wall was considered as having a constant [6−10] value or a variable rate (mass flux). The environment was treated as being uniform, thermally [1−3, 6,11−13] or doubly stratified [14]. This work considers the particular case of a vertical impermeable semi-infinite wall of constant mass flux and temperature embedded in a Newtonian fluid-saturated Darcy mass-stratified porous medium. The scale analysis of the system [15] establishes the two possible successions of heat and mass driven convection regimes that we can encounter along the wall as a function of the process parameters. The finite differences method [16] applied to the numerical model verifies these two possibilities for certain particular parameter sets.

2. MATHEMATICAL MODEL

Figure 1(a) presents the semi-infinite vertical impermeable wall of constant mass flux (m_w) and temperature (T_w), a wall that is embedded in a Newtonian fluid-saturated Darcy porous medium and the coordinate system attached to it. At the right end of the boundary layer, y_∞, the temperature is T_∞, the environment concentration is $C_{\infty,x} = C_{\infty,0} + s_C x$,

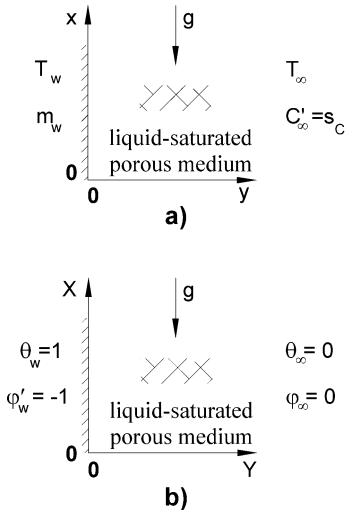

Fig. 1: (a) The vertical wall and the associated coordinate system; (b) the dimensionless domain.

while the dimensional concentration stratification coefficient is $s_C = dC_{\infty,x}/dx$. All the properties are constant except for the fluid density that obeys the Boussinesq approximation. The governing equations:

$$\frac{\partial v}{\partial x}+\frac{\partial u}{\partial y}=0 \tag{1}$$

$$\frac{\partial v}{\partial y}-\frac{\partial u}{\partial x}=\frac{K}{\mu}\left[\rho g\beta_t\frac{\partial T}{\partial y}+\rho g\beta_c\frac{\partial C}{\partial y}\right] \tag{2}$$

$$\frac{\partial T}{\partial t}+v\frac{\partial T}{\partial x}+u\frac{\partial T}{\partial y}=\alpha\left(\frac{\partial^2 T}{\partial x^2}+\frac{\partial^2 T}{\partial y^2}\right) \tag{3}$$

$$\frac{\partial C}{\partial t}+v\frac{\partial C}{\partial x}+u\frac{\partial C}{\partial y}=D\left(\frac{\partial^2 C}{\partial x^2}+\frac{\partial^2 C}{\partial y^2}\right) \tag{4}$$

are solved using the following boundary conditions:

$$u=0,\ T=T_w,\ \frac{\partial C}{\partial y}=-\frac{m_w}{D}=C_{x0}\ \text{at}\ y=0$$

$$v=0,\ T=T_\infty,\ C=C_{\infty,x}\ \text{as}\ y\to\infty$$

$$v=0,\ T=T_\infty,\ C=C_{\infty,0}\ \text{at}\ x=0$$

$$\frac{\partial^2 u}{\partial x^2}=\frac{\partial^2 v}{\partial x^2}=\frac{\partial^2 T}{\partial x^2}=\frac{\partial^2 C}{\partial x^2}=0\ \text{at}\ x=h, \tag{5}$$

where t is the time, u and v are the horizontal and the vertical velocities, ρ is the density, β_t/β_c is the temperature/concentration volumetric expansion coefficients, α/D is the thermal/mass diffusivity, *h* is the height of the computational domain

The definition of the non-dimensional variables:

$$X=\frac{x}{L},\ Y=\frac{y}{L},\ \theta=\frac{T-T_\infty}{T_w-T_\infty},\ \varphi=\frac{C-C_\infty}{m_wL/D},$$

$$\tau=\frac{t\alpha}{L^2},\ U=\frac{u}{\alpha}L,\ V=\frac{v}{\alpha}L \tag{6}$$

lead to the dimensional governing equations:

$$\frac{\partial V}{\partial X}+\frac{\partial U}{\partial Y}=0 \tag{7}$$

$$\frac{\partial V}{\partial Y}-\frac{\partial U}{\partial X}=Ra\left(\frac{\partial\theta}{\partial Y}+N\frac{\partial\varphi}{\partial Y}\right) \tag{8}$$

$$\frac{\partial\theta}{\partial\tau}+V\frac{\partial\theta}{\partial X}+U\frac{\partial\theta}{\partial Y}=\frac{\partial^2\theta}{\partial X^2}+\frac{\partial^2\theta}{\partial Y^2} \tag{9}$$

$$\frac{\partial\varphi}{\partial\tau}+V\frac{\partial\varphi}{\partial X}+VS_C+U\frac{\partial\varphi}{\partial Y}=\frac{1}{Le}\left(\frac{\partial^2\varphi}{\partial X^2}+\frac{\partial^2\varphi}{\partial Y^2}\right) \tag{10}$$

Rayleigh number, $Ra=\left[Kg\beta_t\left(T_w-T_{\infty,0}\right)L^3/\alpha\nu\right]$, Lewis number, $Le=\left(\alpha/D\right)$, the buoyancy ratio, $N=\left[\beta_c\left(C_w-C_{\infty,0}\right)/\beta_t\left(T_w-T_{\infty,0}\right)\right]$, the thermal and the concentration dimensionless stratification parameters: $S_T=\left[s_TL/\left(T_w-T_{\infty,0}\right)\right]$, $S_C=\left[s_CL/\left(m_wL/D\right)\right]$ are defined.

The dimensionless boundary conditions become:

$$U=0,\ \theta=1,\ \partial\varphi/\partial Y=-1\ \text{at}\ Y=0 \tag{11a}$$

$$V=0,\ \theta=\varphi=0\ \text{as}\ Y\to\infty \tag{11b}$$

$$V=0,\ \theta=\varphi=0\ \text{at}\ X=0 \tag{11c}$$

$$\frac{\partial^2 U}{\partial X^2}=\frac{\partial^2 V}{\partial X^2}=\frac{\partial^2\theta}{\partial X^2}=\frac{\partial^2\varphi}{\partial X^2}=0\ \text{at}\ X=H \tag{11d}$$

The conservation equations are analyzed using the scale analysis method in Section 3, while the finite difference method applied to the mathematical model verifies this analysis in Section 4.

3. SCALE ANALYSIS

The scale analysis [15] considers the transient state (section 3.1) as well as the equilibrium state for both the heat driven convection (HDC) regime (section 3.2) and the mass driven convection (MDC) regime (section 3.3).

3.1. Scale analysis of the transient state

In the transient state, the scale analysis of (9) requires the equilibrium of the terms representing the inertia and the diffusion of heat in the horizontal direction: $\partial\theta/\partial\tau\sim\partial^2\theta/\partial Y^2$. The temperature difference registered by the thermal boundary layer is $\Delta T\sim\left(T_w-T_0\right)$ or $\Delta\theta\sim 1$, while $Y\sim\delta_T$ and, consequently, the temperature boundary layer thickness in the transient state is:

$$\delta_T\sim\tau^{1/2} \tag{12}$$

Similarly, considering the equilibrium between the inertia and the horizontal diffusion of the species, in Eq. (10), we obtain: $\partial\varphi/\partial\tau\sim 1/Le\cdot\partial^2\varphi/\partial Y^2$. As $Y\sim\delta_C$, the thickness of the concentration boundary layer, δ_C, is:

$$\delta_C\sim\tau^{1/2}/Le^{1/2} \tag{13}$$

The concentration difference across the concentration boundary layer is: $\Delta C\sim C_{x0}\delta_C\sim C_{x0}\tau^{1/2}/Le^{1/2}$ or $\Delta\varphi\sim\tau^{1/2}/Le^{1/2}$.

Further, assuming that the boundary layer approximation is valid, $\delta_T\ll X$ and $\delta_C\ll X$ (the validity of this assumption is established after Eq.(36)), we neglect the $\partial U/\partial X$ term in (8): $\frac{\partial V}{\partial Y}\sim Ra\cdot(\frac{\partial\theta}{\partial Y})+Ra\cdot N\cdot(\frac{\partial\varphi}{\partial Y})$ and we integrate this equation from $Y=0$ to infinity:

$$V\sim Ra\cdot\left(\Delta\theta\right)+Ra\cdot N\cdot\left(\Delta\varphi\right) \tag{14}$$

The first term on the right hand side of (14) is V_T, the vertical velocity due to the volumetric thermal expansion

$$V_T\sim Ra\cdot\left(\Delta\theta\right)\sim Ra \tag{15}$$

while the second term on the right hand side of (14) is V_C, the vertical velocity due to the volumetric concentration expansion:

$$V_C\sim Ra\cdot N\cdot\left(\Delta\varphi\right)\sim Ra\cdot N\cdot\tau^{1/2}/Le^{1/2} \tag{16}$$

Therefore, the vertical velocity scale becomes:

$$V \sim Ra + Ra \cdot N \cdot \tau^{1/2} / Le^{1/2} \quad (17)$$

An analysis of (17) shows that the velocity component due to the evolution of the concentration field (V_C) increases in time, while the velocity component due to the evolution of the temperature field (V_T) is constant. Consequently, a heat driven convection regime dominates initially at each abscissa, but, if the equilibrium time, τ_{ech}, is bigger than the transition time, τ_{trz}:

$$\tau_{ech} < \tau_{trz} = Le / N^2 \quad (18)$$

A mass driven convection (MDC) regime will attain the equilibrium state at that abscissa. In the MDC regime, as $\Delta\theta \sim 1$ and V is given by (14), the concentration difference across the boundary layer is $\Delta\varphi > 1/N$.

3.2. *Scale analysis of the heat driven convection (HDC) regime*

In the heat driven convection regime, the equilibrium is reached when the heat flux diffused in the Y direction equals the heat flux convected in the X direction: $V \cdot \Delta\theta / X \sim \Delta\theta / \delta_T^2$. Replacing (12) and (15), the temperature field attains the equilibrium state at the moment:

$$\left(\tau_{ech,T}\right)_T \sim X / Ra \quad (19)$$

At this moment, according to (12), the boundary layer thickness is:

$$\left(\delta_{ech,T}\right)_T \sim \left(X / Ra\right)^{1/2} \quad (20)$$

The equilibrium time, $\left(\tau_{ech,T}\right)_T$, is bigger than the transition time, τ_{trz}, if:

$$X_{trz} = Ra \cdot Le / N^2 < X \quad (21)$$

Scale analysis of the concentration field in the HDC regime

The analysis of the concentration field in the HDC regime starts with the analysis of the vertical velocity terms: VS_C and $V \cdot \partial\varphi / \partial X$, in the species conservation equation, Eq. (10). The VS_C term is dominant if $S_C > \tau^{1/2} / Le^{1/2} / X$ or

$$\tau < \tau_s = S_C^2 X^2 Le \quad (22)$$

Equation (22) states that, at the beginning, when $\tau < \tau_s$, the VS_C term is dominant but, in time, this situation remains unchanged or not depending on the relative magnitude of τ_s, τ_{trz}, $\left(\tau_{ech,T}\right)_T$ and the equilibrium time of the concentration field. This later variable is established as follows:

a) If the $V \cdot \partial\varphi / \partial X$ term is greater than the VS_C term in Eq. (10), then the scale analysis reveals that:

$$V \cdot \partial\varphi / \partial X \sim \left(\partial^2\varphi / \partial Y^2\right) / Le \quad (23)$$

and, after replacing Eq. (13) and Eq. (15) in Eq. (23), we find the order of magnitude of the equilibrium time of the concentration field:

$$\left(\tau_{ech,C}\right)_T \sim X / Ra \quad (24)$$

As we can notice, for this situation, the temperature and the concentration fields attain the equilibrium state in the same moment as $\left(\tau_{ech,T}\right)_T$, Eq.(19), and $\left(\tau_{ech,C}\right)_T$, Eq.(24), have the same form.

The concentration boundary layer thickness is

$$\left(\delta_{ech,C}\right)_T \sim \left[X / (Ra \cdot Le)\right]^{1/2} \quad (25)$$

b) If the $V \cdot S_C$ term is the dominant vertical convection term in Eq.(10), then the scale analysis reveals that:

$$V \cdot S_C \sim \left(\partial^2\varphi / \partial Y^2\right) / Le \quad (26)$$

Using Eqs. (13) and (15), we conclude that the equilibrium time is $\left(\tau_{ech,Sc}\right)_T \sim \left(1 / Ra / S_C\right)^2 / Le$ and that the magnitude of the equilibrium concentration boundary layer thickness is:

$$\left(\delta_{ech,St}\right)_C \sim 1 / (Ra \cdot S_C \cdot Le) \quad (27)$$

Further, the equilibrium time $\left(\tau_{ech,,Sc}\right)_T$ will be compared to τ_{trz} and τ_s:

b1) the equilibrium time $\left(\tau_{ech,,Sc}\right)_T$ is smaller than the transition time, τ_{trz}, if:

$$Ra \cdot S_C \cdot Le / N > 1 \quad (28)$$

b2) the possibility to have $\left(\tau_{ech,Sc}\right)_T < \tau_s$ is restricted to the domain defined bellow:

$$X > 1 / \left(Ra \cdot S_C^2 \cdot Le\right) = X_s \quad (29)$$

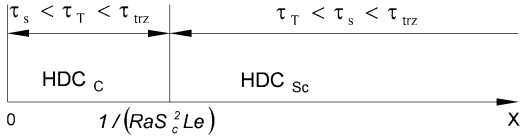

a) $Ra \cdot Le \cdot S_C / N \geq 1$

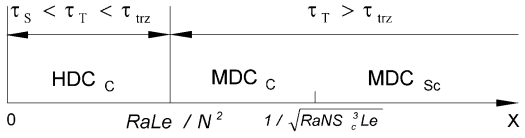

b) $Ra \cdot Le \cdot S_C / N < 1$

Fig. 2: The heat and mass driven natural convection regimes sequence. a) $Ra \cdot Le \cdot S_C / N \geq 1$; b) $Ra \cdot Le \cdot S_C / N < 1$.

Two distinct situations appear:

1. If Eq. (28) is valid, then the heat→mass driven convection transformation is not taking place because $X_s < X_{trz}$ and at the X_{trz} abscissa, the velocity is already settled to a constant value: $V \sim Ra\left[1 + N / (RaS_C Le)\right]$, where $V_T \sim Ra$ is the greater term. The regimes succession is presented by Fig. 2a: HDC_C — HDC_{Sc}.

2. If Eq. (28) is not valid, $X_s > X_{trz}$ and the regimes succession: HDC_C — MDC_C — MDC_{Sc} is encountered (Figure 2b). In order to establish the abscissa where the MDC_C— MDC_{Sc} transition is taking place, the scale analysis of the MDC regime is presented in the next section.

3.3. Scale analysis of the mass driven convection (MDC) regime

MDC_{Sc} regime (the $V \cdot S_C$ term is dominant) and **MDC_C** regime (the $V \cdot \partial\varphi / \partial X$ term is dominant) will be treated separately.

3.3.1. MDC_{Sc} regime

The equilibrium state in the MDC_{Sc} regime is reached at the moment when the diffusion of mass away from the wall, in the Y direction, equals the convection of mass expressed by the $V \cdot S_C$ term:

$$V \cdot S_C \sim \left(\partial^2 \varphi / \partial Y^2\right) / Le \tag{30}$$

Using Eq. (13) and Eq. (16) in Eq. (30), we obtain the equilibrium time and boundary layer thickness:

$$\left(\tau_{ech,Sc}\right)_c \sim 1/\left(RaNS_C\right) \tag{31}$$

$$\left(\delta_{ech,Sc}\right)_c \sim \sqrt{1/\left(RaNS_C Le\right)} \tag{32}$$

This state of equilibrium is attained before the transition $MDC_{Sc} \rightarrow MDC_C$ if $\left(\tau_{ech,Sc}\right)_C < \tau_s$ or

$$X > 1/\sqrt{RaNS_C^3 Le} \tag{33}$$

This is the condition that separates MDC_C and MDC_{Sc} regimes in Fig. 2(b).

3.3.2. MDC_C regime

If the $V \cdot \partial\varphi / \partial X$ term is dominant, the equilibrium state is characterized by: $V \cdot \Delta\varphi / X \sim 1/Le \cdot \Delta\varphi / \delta_C^2$. The equilibrium time and concentration boundary layer thickness are:

$$\left(\tau_{ech,C}\right)_V \sim \left(XLe^{1/2} / Ra / N\right)^{2/3} \tag{34}$$

$$\left(\delta_{ech,T}\right)_T \sim \left(XLe^{1/2} / Ra / N\right)^{1/3} \tag{35}$$

Scale analysis of the temperature field in the MDC regime. The scale analysis of Eq. (9) reveals that $V \cdot \partial\theta / \partial X \sim \partial^2\theta / \partial Y^2$. Using Eq. (12) and Eq. (16), the time when the temperature field attains the equilibrium is $\left(\tau_{ech,T}\right)_C \sim \left(XLe^{1/2} / Ra / N\right)^{2/3}$. The temperature boundary layer thickness is:

$$\left(\delta_{ech,T}\right)_C \sim \left(XLe^{1/2} / Ra / N\right)^{1/3} \tag{36}$$

The validity of this scale analysis imposes:

- if $Ra \cdot S_C \cdot Le / N \geq 1$: $\left(\delta_{ech,T}\right)_T \ll X$ and $\left(\delta_{ech,C}\right)_T \ll X$ for $X = 1/\left(RaS_C^2 Le\right) = X_s$. These set of conditions requires: $S_C \ll 1$ and $X > 1/Ra$ (this condition defines a diffusion region for low values of X [17]));
- if $Ra \cdot S_C \cdot Le / N < 1$: $\left(\delta_{ech,T}\right)_T \ll X$ and $\left(\delta_{ech,C}\right)_T \ll X$ for $X = RaLe / N^2$ and $\left(\delta_{ech,C}\right)_C \ll X$ and $\left(\delta_{ech,T}\right)_C \ll X$ for $X = 1/\sqrt{RaNS_C^3 Le}$. These set of conditions requires: $X > 1/Ra$ and $S_C Le^{1/2} \ll 1$.

4. NUMERICAL MODELING

Using the stream function definition of the velocity field: $U = -\partial\Psi / \partial X$ and $V = \partial\Psi / \partial Y$, the dimensionless governing equations become:

$$\frac{\partial^2\Psi}{\partial Y^2} + \frac{\partial^2\Psi}{\partial X^2} = Ra \cdot \left(\frac{\partial\theta}{\partial Y} + N\frac{\partial\varphi}{\partial Y}\right) \tag{37}$$

$$\frac{\partial\theta}{\partial\tau} + \frac{\partial\Psi}{\partial Y}\frac{\partial\theta}{\partial X} - \frac{\partial\Psi}{\partial X}\frac{\partial\theta}{\partial Y} = \frac{\partial^2\theta}{\partial X^2} + \frac{\partial^2\theta}{\partial Y^2} \tag{38}$$

$$\frac{\partial\varphi}{\partial\tau} + \frac{\partial\Psi}{\partial Y}\frac{\partial\varphi}{\partial X} + S_C\frac{\partial\Psi}{\partial Y} - \frac{\partial\Psi}{\partial X}\frac{\partial\varphi}{\partial Y} = \frac{1}{Le}\left(\frac{\partial^2\varphi}{\partial X^2} + \frac{\partial^2\varphi}{\partial Y^2}\right) \tag{39}$$

while the dimensionless boundary conditions are:

$$\Psi = 0,\ \partial\varphi / \partial Y = -1,\ \theta = 1 \text{ at } Y = 0 \tag{40a}$$

$$\frac{\partial\Psi}{\partial Y} = 0,\ \theta = \varphi = 0 \text{ as } Y = L \tag{40b}$$

$$\Psi = 0,\ \theta = \varphi = 0 \text{ at } X = 0 \tag{40c}$$

$$\frac{\partial^2\psi}{\partial X^2} = \frac{\partial^3\psi}{\partial X^3} = \frac{\partial^2\theta}{\partial X^2} = \frac{\partial^2\varphi}{\partial X^2} = 0 \text{ at } X = H \tag{40d}$$

The governing equations, (37) − (39), subjected to the boundary conditions, (40), were solved using the finite difference method, the higher order hybrid scheme [16]. The program was tested using the results published in the literature [18-20].

5. RESULTS AND DISCUSSIONS

The HDC_C—HDC_{Sc} regime succession of Fig. 2a is exemplified for the following parameter set: $Ra = 200$, $N = 5.0$, $Le = 1$ and $S_C = 0.05$. In this case, $Ra \cdot S_C \cdot Le / N = 2$ and $1/\left(Ra \cdot S_C^2 \cdot Le\right) = 2$. Figure 3 presents the dimensionless temperature (Fig. 3(a)), concentration (Fig. 3(b)), stream function (Fig. 3(c)) and $\left(\partial\varphi / \partial X\right) / S_C$ (Fig. 3(d)) fields. The 0.4×10.0 computational domain was discretised using 41×1001 points. A relative error of each variable in each point of 10^{-6} was used to stop the iterative process developed with a time step of 3.0×10^{-4}. The concentration field in Fig. 3(b) does not exceed the $1/N = 0.2$ value across the boundary layer which indicates that there is no HDC—MDC transition. Figure 3(d) reveals that the HDC_C—HDC_{Sc} transition takes place at the 0.6 abscissa.

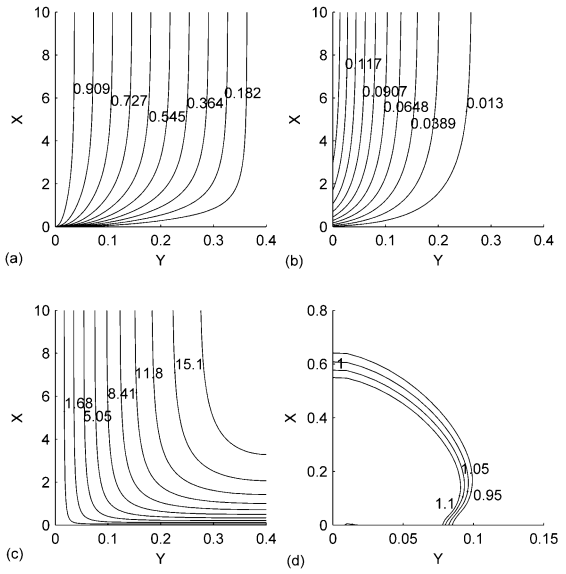

Fig. 3: (a) θ, (b) φ, (c) Ψ and (d) $(\partial\varphi/\partial X)/S_C$ fields. $Ra = 200$, $N = 5.0$, $Le = 1$ and $S_C = 0.05$.

Figure 4 presents the variations of dimensionless (Fig. 4(a)-(c)) as well as scaled dimensionless (Fig. 4(d)-(f)) temperature, concentration and vertical velocity, respectively, at three abscissas in the HDC_C region: 0.2, 0.4 and 0.6. The comparison of the un-scaled and the scaled plots shows clearly the validity of the scale analysis.

Figure 5 presents the variations of the dimensionless temperature, concentration and vertical velocity (Fig. 5(a)-(c)) at three abscissas in the HDC_{Sc} region: 4.0, 6.0 and 8.0 as well as scaled temperature, concentration and vertical velocity variations (Fig. 5(a)-(c)) for the same three abscissas revealing, again, the validity of the scale analysis.

The HDC_C—MDC_C—MDC_{Sc} succession presented by Fig. 2(b) is exemplified using the parameter set: $Ra = 100$, $N = 10.0$, $Le = 1$ and $S_C = 0.02$. The computational domain has a 0.6×20.0 size, the discretisation grid uses 61×2001 points, the relative error of each variable in each point at the end of the iterative process is lower than 10^{-6}, while the time step is 3.0×10^{-4}. Figure 6 presents θ (Fig. 6(a)), $\varphi/(1/N)$ (Fig. 6(b)), ψ (Fig. 6(c)) and $(\partial\varphi/\partial X)/S_C$ (Fig. 6(d)) fields for this particular parameter set. We notice that the HDC_C—MDC_C regime transition takes place at an abscissa of 0.6, while the MDC_C— MDC_{Sc} transition is taking place at the 2.4 abscissa.

Further, each of the three regions (HDC_C, MDC_C and MDC_{Sc}) was analyzed using three cuts:
- Fig. 7: 0.2, 0.4, 0.6 abscissas—the HDC_C region;
-Fig. 8: 1.2, 1.6 and 2.0 abscissas—the MDC_C region;
-Fig. 9: 13.0, 15.0 and 17.0 abscissas—MDC_{Sc} region.

Dimensionless and scaled dimensionless temperature, concentration and vertical velocity plots were drawn for each abscissa proving the validity of the scale analysis results.

The figures (3)−(9) verify the two regimes succession found by the scale analysis of the conservation equations of the system.

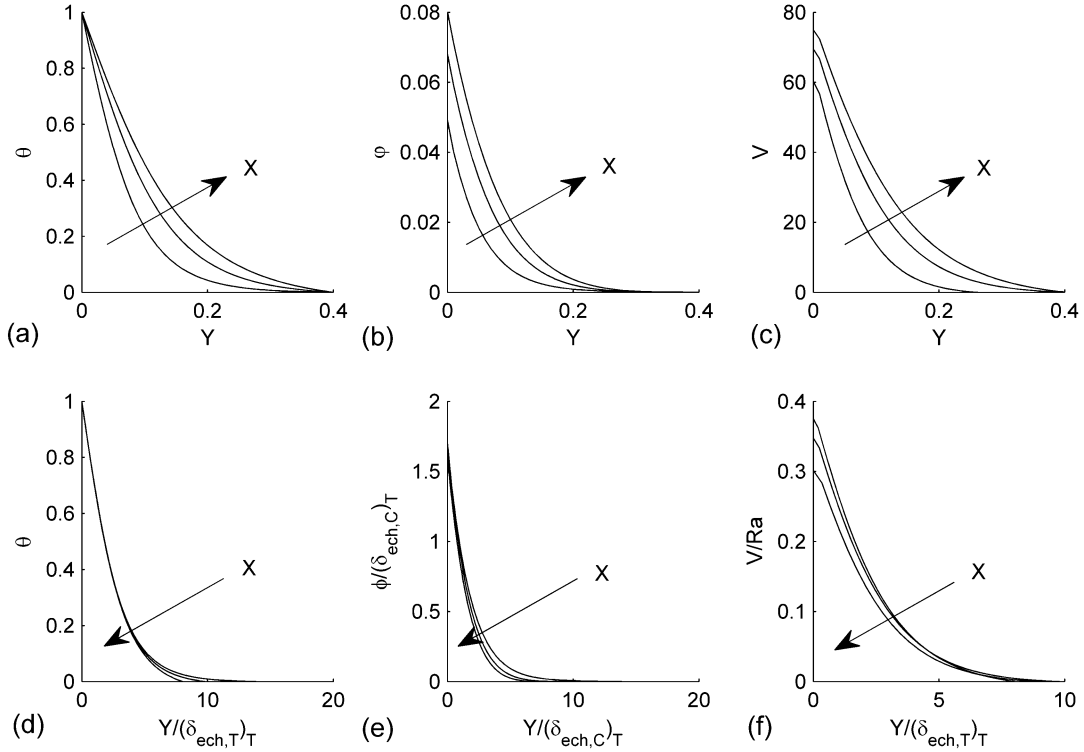

Fig. 4: (a) θ, (b) φ and (c) V variations as a function of Y and the scaled (d) θ, (e) φ and (f) V variations as a function of scaled ordinate, for the abscissas: 0.2, 0.4 and 0.6; $Ra = 200$, $N = 5.0$, $Le = 1$, $S_C = 0.05$.

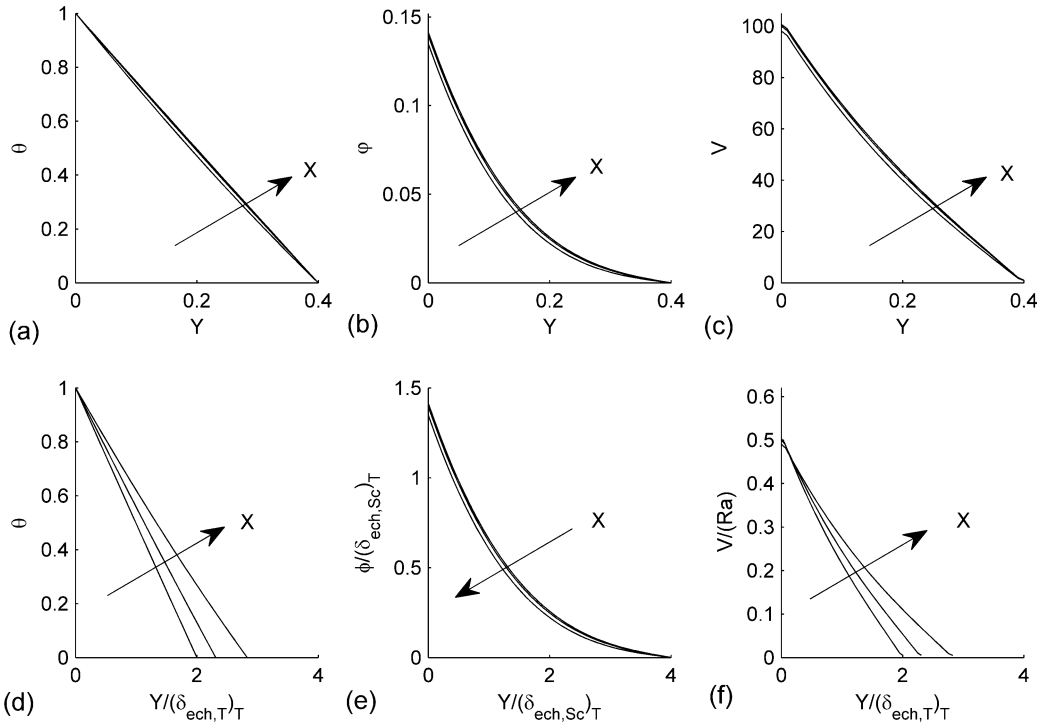

Fig. 5: (a) θ, (b) φ and (c) V variations as a function of Y and the scaled (d) θ, (e) φ and (f) V variations as a function of scaled ordinate, for three abscissas: 4.0, 6.0 and 8.0; $Ra = 200$, $N = 5.0$, $Le = 1$ and $S_C = 0.05$.

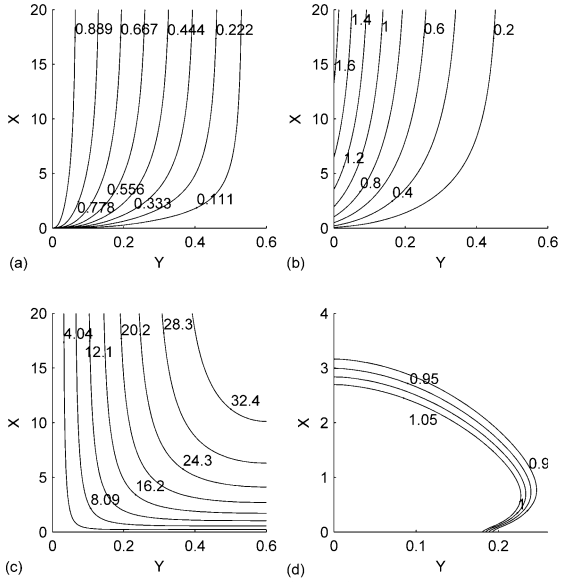

Fig. 6: (a) θ, (b) $\varphi/(1/N)$, (c) ψ and (d) $(\partial\varphi/\partial X)/S_C$ fields. $Ra = 100$, $N = 10.0$, $Le = 1$ and $S_C = 0.02$.

6. CONCLUSIONS

This paper presents the analysis of the natural convection triggered by a constant mass flux and temperature vertical impermeable wall situated in a fluid saturated Darcy mass stratified porous medium.

The scale analysis of the system reveals two possible maps of the heat and mass driven natural convection processes that attain the equilibrium state along the wall: if $Ra \cdot Le \cdot S_C / N \geq 1$, then a HDC_C—HDC_{Sc} sequence is encounter along the wall; otherwise a HDC_C—MDC_C—MDC_{Sc} is registered.

The finite difference method is used to verify these two maps for two particular parameter sets.

These results bring a new understanding of the natural convection that takes place in the boundary layer of a vertical wall of constant mass flux and temperature, a wall that is embedded in a Darcy mass stratified porous medium.

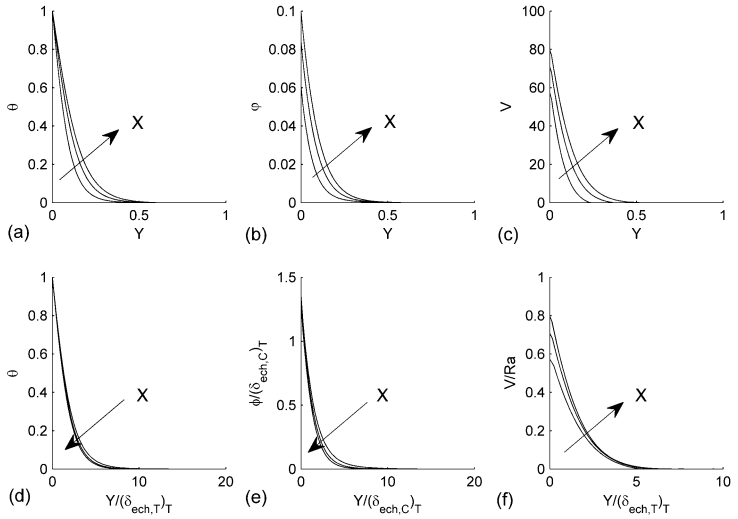

Fig. 7: (a) θ, (b) φ and (c) V variations as a function of Y and the scaled (d) θ, (e) φ and (f) V variations as a function of scaled ordinate, for the abscissas: 0.2, 0.4 and 0.6. $Ra = 100$, $N = 10.0$, $Le = 1$ and $S_C = 0.02$.

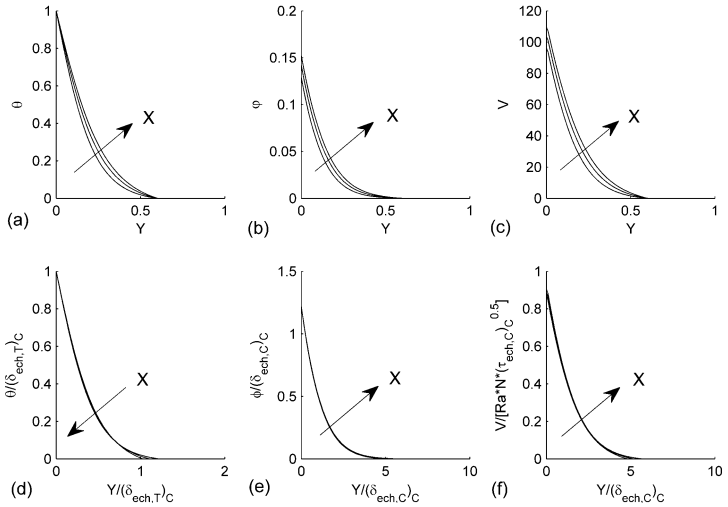

Fig. 8: (a) θ, (b) φ and (c) V variations as a function of Y and the scaled (d) θ, (e) φ and (f) V variations as a function of scaled ordinate, for three abscissas: 1.2, 1.6 and 2.0. $Ra = 100$, $N = 10.0$, $Le = 1$ and $S_C = 0.02$.

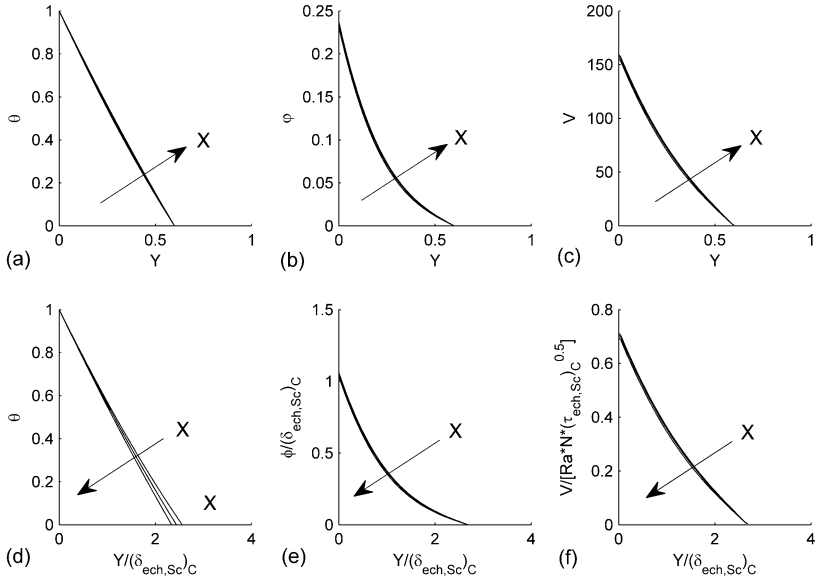

Fig. 9: (a) θ, (b) φ and (c) V variations as a function of Y and the scaled (d) θ, (e) φ and (f) V variations as a function of scaled ordinate, for three abscissas: 13.0, 15.0 and 17.0. $Ra = 100$, $N = 10.0$, $Le = 1$, $S_C = 0.02$.

REFERENCES

[1] **C. 'O-K. Chen, C.-R. Lin**, *Natural convection from an isothermal vertical surface embedded in a thermally stratified high-porosity medium*, International Journal of Engineering Science 33 (1), 1995, pag. 131−138.

[2] **K. Tewari. P. Singh**, *Natural convection in a thermally stratified fluid saturated porous medium*, International Journal of Engineering Science 30 (8), 1992, pag. 1003−1007.

[3] **C.-I. Hung, C.-H. Chen, C-B. Chen**, *Non-Darcy free convection along a nonisothermal vertical surface in a thermally stratified porous medium,* International Journal of Engineering Science 37 (4), 1999, pag. 477−495.

[4] **F.C. Lai**, *Non-Darcy natural convection from a line source of heat in saturated porous medium*, International Communications in Heat and Mass Transfer 18 (4), 1991, pag. 445−457.

[5] **Z. H. Kodah, A. M. Al-Gasem**, *Non-Darcy mixed convection from a vertical plate in saturated porous media-variable surface heat flux*, Heat and Mass Transfer 33 (5−6), 1998, pag. 377−382.

[6] **D. Angirasa, G. P. Peterson**, *Natural convection heat transfer from an isothermal vertical surface to a fluid saturated thermally stratified porous medium*, International Journal of Heat and Mass Transfer 40 (18), 1997, pag. 4329−4335.

[7] **J.-Y. Jang, J.-R. Ni**, *Transient free convection with mass transfer from an isothermal vertical flat plate embedded in a porous medium*, International Journal of Heat and Fluid Flow 10 (1) (1989) 59−65.

[8] **A. Bejan, K. R. Khair**, *Heat and mass transfer by natural convection in a porous medium*, International Journal of Heat and Mass Transfer 28 (5) (1985) 909−918.

[9] **D. Angirasa, G. P. Peterson**, I. Pop, *Combined heat and mass transfer by natural convection with opposing buoyancy effects in a fluid saturated porous medium*, International Journal of Heat and Mass Transfer 40 (12) (1997) 2755−2773.

[10] **I. Pop, H. Herwig**, *Transient mass transfer from an isothermal vertical flat plate embedded in a porous medium*, International Communications in Heat and Mass Transfer 17 (6), 1990, pag. 813−821.

[11] **C. Allain, M. Cloitre, A. Mongruel**, *Scaling in flows driven by heat and mass convection in a porous medium*, Europhysics Letters 20 (4), 1992, pag. 313−318.

[12] **I. Y. Hussain, B. K. Raheem**, *Natural convection heat transfer from a plane wall to thermally stratified porous media*, International Journal of Computer Applications 65 (1), 2013, pag. 42−49.

[13] **P. Singh, K. Sharma**, *Integral method to free convection in thermally stratified porous medium*, Acta Mechanica 83 (3−4), 1990, pag. 157−163.

[14] **P. A. Lakshmi Narayana, P. V. S. N. Murthy**, *Free convective heat and mass transfer in a doubly stratified non-darcy porous medium*, ASME Journal of Heat Transfer 128 (11), 2006, pag. 1204−1212.

[15] **A. Bejan**, *Convection Heat Transfer*, second ed., Wiley, New York, 1995, pag. 18−21, pag. 535-539.

[16] **J. C. Tannehill, D. A. Anderson, R. H. Pletcher**, *Computational Fluid Mechanics and Heat Transfer*, second ed., Taylor&Francis, Washington, 1997, pag. 45−70.

[17] **S. W. Armfield, J. C. Patterson**, *W. Lin, Scaling investigation of the natural convection boundary layer on an evenly heated plate*, International Journal of Heat and Mass Transfer 50 (7-8), 2007, pag. 1592-1602.

[18] **O.V. Trevisan, A. Bejan**, *Natural convection with combined heat and mass transfer buoyancy effects in a porous medium*, International Journal of Heat and Mass Transfer 28 (8), 1985, pag. 1597-1611.

[19] **D. Getachew, D. Poulikakos, W. J. Minkowycz**, *Double diffusion in a porous cavity saturated with non-Newtonian fluid*, Journal of Thermophysics and Heat Transfer 12 (3), 1998, pag. 437−446.

[20] **R. Bennacer, A. Tobbal, H. Beji, P. Vasseur**, *Double diffusive convection in a vertical enclosure filled with anisotropic porous media*, International Journal of Thermal Sciences 40 (1), 2001, pag. 30-41.